Original Article
Diagnostic report of high-resolution magnetic susceptibility weighted imaging for cerebral vascular amyloid angiopathy-related microbleeds

Qingliang Feng[1*], Sheng Gao[1*], Yan Liu[2], Zhiliang He[3], Jiangwei Xie[1]

Departments of [1]Radiology, [2]Health Management Center, Linyi Central Hospital, Linyi, Shandong Province, China; [3]Department of Radiology, Dezhou People's Hospital, Dezhou, Shandong Province, China. *Equal contributors and co-first authors.

Abstract: Objective: To determine the value of susceptibility weighted imaging (SWI) in the differential diagnosis of cerebral amyloid angiopathy (CAA)-related microbleeds. Methods: The clinical data of 33 patients with highly suspected CAA-related microbleeds were retrospectively analyzed. All subjects underwent conventional T1-weighted spin-echo imaging, T2-weighted fast spin-echo imaging and SWI. The investigators evaluated the diagnostic value of different magnetic resonance imaging (MRI) sequences by assessing the imaging features of CAA-related microbleeds. Results: The microbleeds of the subjects were mainly located in the cerebral cortex and subcortical regions. Fourteen cases were also found to have chronic hematoma remote hemorrhage in the cerebellar hemisphere. Seven cases had subacute or remote hemorrhage in the basal ganglia, 3 cases in the thalamus and another 3 cases in the brain lobe. In the conventional MRI sequences, CAA-related microbleeds manifested as low or intermediate signals in T1 weighted imaging (T1WI); in some cases short T1 signals could be seen. In T2 weighted imaging (T2WI), the lesions were heterogeneous pattern with mixed areas of high and low signal intensity. In the SWI sequence, more hemorrhagic foci were seen, showing low signal areas with clear margins. And punctate or patchy high signals were seen in the center of some lesions. The count of microbleeds showed by SWI was significantly higher than that of T1WI or T2WI (P<0.01). The Kappa consistency test showed that the SWI sequence was consistent with T2WI and T1WI sequences, and the Kappa values were 0.63 and 0.54, respectively. The P values were less than 0.01. Conclusion: For patients with cerebral vascular amyloid microbleeds, high-resolution SWI can achieve better diagnostic results, showing clear lesions with higher detection sensitivity.

Keywords: High-resolution susceptibility weighted imaging, cerebral amyloid angiopathy, microbleeds, magnetic resonance imaging

Introduction

Susceptibility weighted imaging (SWI) is a high-resolution three-dimensional technique that uses not only the magnitude information of magnetic resonance imaging (MRI) signals, but also the phase information compared with the traditional T2* weighted gradient-recalled echo imaging (GRE) [1]. The phase and magnitude data are combined in subsequent processing steps by minimum intensity projection technique to increase the sensitivity or contrast of paramagnetic tissue, which includes vein structure and cerebral microbleeds (CMB) [2].

Cerebral amyloid angiopathy (CAA) is associated with perivascular rupture, which is caused by deposition of amyloid β-protein in blood vessels. Previous autopsies have shown that the prevalence of CAA in Alzheimer's disease is 70% to 90% [3]. CAA is an important cause of intracerebral hemorrhage (ICH) in the elderly, accounting for 10-20% of spontaneous ICH. With the increase of life expectancy, it's expected that the prevalence of CAA-related ICH will follow [4]. This study evaluates the value of SWI in the diagnosis of CAA-related microbleeds.

Materials and methods

Patients

The clinical data of 33 patients with highly suspected CAA-related microbleeds were retrospectively analyzed. The patients were admitted to Linyi Central Hospital from July 2015 to

Table 1. Modified Boston diagnostic criteria

Diagnosis	Criteria
Definite CAA	Full post-mortem examination reveals lobar, cortical, or cortical/subcortical hemorrhage and pathological evidence of severe cerebral amyloid angiopathy
Probable CAA with supporting pathological evidence	Clinical data and pathological tissues (evacuated hematoma or cortical biopsy specimens) demonstrate a hemorrhage as mentioned above and some degree of vascular amyloid deposition
Probable CAA	A. Patient is 55 years or older B. Appropriate clinical history C. MRI or CT findings demonstrate: Multiple hemorrhages restricted to the lobar, cortical, or cortico-subcortical regions without another cause, or a single lobar, cortical, or cortico-subcortical hemorrhage and focal or disseminated cortical superficial siderosis without another cause
Possible CAA	A. Patient is 55 years or older B. Appropriate clinical history C. MRI or CT findings demonstrate: A single lobar, cortical, or cortico-subcortical hemorrhage without another cause, or focal or disseminated cortical superficial siderosis without another cause

Note: CAA, Cerebral amyloid angiopathy.
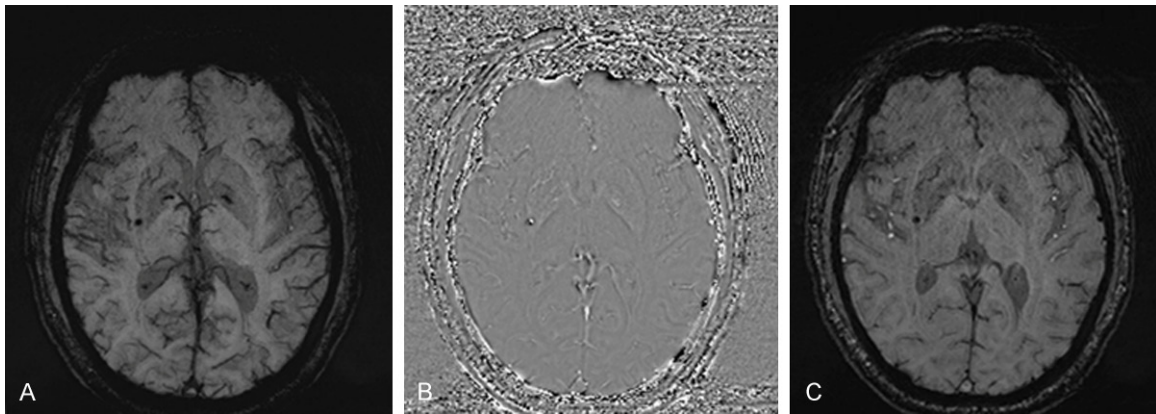
Figure 1. Cerebral microbleeds. A: T1WI, T1 weighted imaging; B: T2WI, T2 weighted imaging; C: SWI, susceptibility weighted imaging.

July 2018. This study was approved by the ethics committee of Linyi Central Hospital. Inclusion criteria: Patients were diagnosed with CAA according to Modified Boston Criteria (see **Table 1**) [5]; patients had provided written informed consent; patients underwent MRI examination including T1WI, T2WI and SWI; patients were at their first attack (**Figure 1**). Exclusion criteria: Patients had intracranial space-occupying lesions; patients had ICH caused by other reasons such as hypertension, trauma, and vascular malformation.

Methods

The Achieva 3.0 T-type superconducting MRI system produced by Philips was used to perform high-resolution SWI and conventional MRI sequences, including T1-weighted spin-echo imaging and T2-weighted fast spin-echo imaging. The patient's head was fixed with a sponge pad before examination to avoid motion artifacts. The SWI parameters were as follows: TR = 34 ms, TE = 49 ms, slice thickness = 6 mm, slice gap = 1 mm, FOV = 24 cm * 24 cm, matrix = 256 * 256. The acquired images were transmitted to the Achieva MR System Release 2.6.3.6 workstation for analysis. The phase mask and magnitude images were generated simultaneously, and the SWI images were acquired through low-pass filtering, phase masking, multiple constant multiplications and minimum intensity projection.

Observation indicators

The images of this study were evaluated by two experienced MRI diagnosticians. The evalua-

Table 2. Number of cases of each sequence based on the Likert scale (n)

Sequence	Cases	5 points	4 points	3 points	2 points	1 point
T1WI	33	4	8	7	8	6
T2WI	33	5	7	8	9	4
SWI	33	7	9	8	7	2

Note: T1WI, T1 weighted imaging; T2WI, T2 weighted imaging; SWI, susceptibility weighted imaging.

tion contents mainly included image quality, location and the number of hemorrhagic foci. The image quality was graded according to the Likert scale: very clear = 5 points; clear = 4 points; fair = 3 points; bad = 2 points; very bad = 1 point. The images with a quality rating of less than 3 were discarded.

Statistical analysis

The data were analyzed using STATA 14.0 software. Enumeration data are expressed as number (n); quantitative values were expressed as mean ± sd. Differences between groups were compared using paired t-tests, χ^2 tests or Kruskal-Wallis tests; and the diagnostic consistency was determined by Kappa tests. The statistical significance level α = 0.05 with a correction for multiple comparisons (α/3 = 0.017).

Results

General information

The age range of the 33 patients is 59-87 years with an average of 67.9±7.6 years. There are 17 males and 16 females. The microbleeds were mainly located in the cerebral cortex and subcortical areas. Except the microbleed lesions, 14 cases were also found to have remote hemorrhage in the cerebellum. Seven cases had subacute or remote hemorrhage in the basal ganglia, 3 cases in the thalamus and another 3 cases in the brain lobe.

Image quality

In the conventional MRI sequence, CAA-related microbleeds manifested as low or intermediate signals in T1 weighted imaging (T1WI); in some cases short T1 signals could be seen. In T2 weighted imaging (T2WI), the lesions were a heterogeneous pattern with mixed areas of high and low signal intensity. The count of microbleeds showed by SWI was significantly

higher than that of T1WI or T2WI, presenting a typical spotted or patchy low signal area.

The number of cases of each sequence based on the Likert scale is shown in **Table 2**. Statistical analysis showed χ^2 = 2.375 and P = 0.3049; the difference among the three sequences was not significant. The proportion of images with image quality equal to or greater than 3 points were 57.58%, 60.61% and 72.73% for the three sequences, respectively. There was no significant difference among the three groups (χ^2 = 1.8333, P = 0.40).

Distribution and count of microbleed lesions

The distribution and count of microbleed lesions on qualified T1WI, T2WI and SWI images are shown in **Table 3**. The microbleeds were mostly distributed in the cortical and subcortical areas. There was no statistically significant difference in distribution of the microbleeds (χ^2 = 1.95, P = 0.98). The mean number of microbleeds shown by T1WI, T2WI and SWI were 14.95±3.26, 16.60±4.11 and 22.42±4.72, respectively. The paired t-test showed significant differences between the three sequences (all P<0.01).

Diagnostic consistency

Seventeen patients with both qualified SWI and T2WI images were selected. The diagnostic results of the two sequences were examined using the Kappa consistency test. Statistics showed that Kappa = 0.63 and P<0.01, indicating the consistency of SWI and T2WI was good. Similarly, 15 patients with both qualified SWI and T1WI images were subject to the Kappa consistency test. The results showed Kappa = 0.54 and P<0.01, indicating the consistency was good. See **Tables 4** and **5**.

Discussion

CMB are rounded micro-hemosiderin deposits around blood vessels that are common in elderly patients and associated with neuropsychiatric disorders. CAA involves cerebral vascular amyloid deposition, which is classified into several types according to the amyloid involved, among which sporadic amyloid β-protein type in

Table 3. Distribution and count of microbleed lesions on qualified T1WI, T2WI and SWI images (n)

Sequence	Number of cases	Cortico-subcortical	Basal ganglia	Thalamus	Cerebellum	Brain stem	Total
T1WI	19	268	3	3	4	6	284
T2WI	20	309	5	4	6	8	332
SWI	24	495	7	8	11	17	538

Note: T1WI, T1 weighted imaging; T2WI, T2 weighted imaging; SWI, susceptibility weighted imaging.

Table 4. Display of brain microbleeds by three sequences (n)

Sequence		T1WI		T2WI	
		Positive	Negative	Positive	Negative
SWI	Positive	223	71	279	83
	Negative	25	116	8	142

Note: T1WI, T1 weighted imaging; T2WI, T2 weighted imaging; SWI, susceptibility weighted imaging.

Table 5. Kappa consistency test

Sequences	Consistency	Kappa	Standard error	Z	P
SWI/T1WI	77.93%	0.54	0.05	11.46	<0.01
SWI/T2WI	82.23%	0.63	0.04	14.89	<0.01

Note: T1WI, T1 weighted imaging; T2WI, T2 weighted imaging.

CAA is most common in elderly and Alzheimer's disease patients [6]. CAA can cause hemorrhagic lesions, ischemic lesions, and subacute leukoencephalopathy.

The causes of CMB are complex, which mainly include hypertension, cerebral ischemia, and CAA. CMB also may be caused by infective endocarditis (IE), thrombotic thrombocytopenic purpura, traumatic brain injury, subcortical infarction, and leukoencephalopathy [7-9]. Sparacia et al. found 91 CMB lesions from 15 patients with end-stage organ failure, 59 (64.84%) were supratentorial lobar distribution, 17 (18.68%) were supratentorial non-lobar distribution, and the remaining 15 (16.48%) were distributed subtentorially [10]. Malhotra et al. found that CMBs in IE affects every part of the brain, especially the cerebellum; and the distribution is different from the pattern in hypertension or CAA. In addition, subarachnoid hemorrhage or deposition of hemosiderin in the meninges are also common in IE [11]. Sparacia used SWI to investigate the relationship between cerebrospinal fluid biomarkers (amyloid β-protein and phosphorylated tau 181 protein levels) and CMBs or cognitive function decline in patients with Alzheimer's disease. A total of 296 microbleeds were observed in 54 patients, of which 38 (70.37%) showed lobar distribution, 13 (24.07%) were non-lobar distribution, and the remaining 3 (5.56%) were mixed distribution; suggesting CMBs in patients with Alzheimer's disease were mainly distributed in the brain lobe, and the number of CMBs in the brain was positively correlated with age, course of disease and cognitive functional declines [12].

Conventional MRI can show non-specific white matter lesions, multifocal cerebral infarction, or brain atrophy. However, CMBs associated with white matter lesions are difficult to differentiate. Although positron emission tomography (PET) can detect CAA through amyloid-binding ligands, such as Pittsburgh Compound B, it does not distinguish between vascular and parenchymal amyloid deposition. Gradient echo (GE) imaging is considered to be a method of detecting hemorrhagic changes in CAA [13]. However, nearly 25% of CAA patients do not show CMBs in $T2^*$ GE sequence [14]. Malhotra et al. studied 66 IE patients who had CAA at the same time, he found that in 11 (16.67%) patients, CMB was the only neuroimaging abnormality, and most CMBs measured between 1 and 3mm. Within that size range, many CMBs can be detected by SWI but not by GRE $T2^*$ [11]. SWI is very sensitive to paramagnetic substances such as deoxygenated blood, blood products, iron and calcium. SWI obtains a three-dimensional reconstruction image of intracerebral vein, which can detect bleeding as early as 6 hours, and can reliably detect acute intraparenchymal hemorrhage and subarachnoid hemorrhage. SWI can also detect early hemorrhagic signs in the infarction, and help understand the cerebral hemodynamics after stroke, which is helpful for diagnosis of cerebral venous thrombosis. This sequence is useful for detecting microbleeds in various situations,

such as vasculitis, autosomal dominant arterial disease, subacute infarction and leukoencephalopathy, amyloid angiopathy, and Binswanger's disease. This sequence also helps to diagnose vascular malformations and perinatal cerebral vascular damage. CMBs appear as <5 mm low signal points in the SWI due to the enhanced $T2^*$ effect of paramagnetic substances such as hemosiderin or deoxyhemoglobin [15]. CAA-related inflammation (CAA-ri) is a rare and treatable variant of CAA that lacks specific imaging and clinical features, previously requiring an invasive brain biopsy to confirm. Kusakable et al. reported a CAA-ri patient with CT showing low-density lesions in the right occipital cortex. MRI showed a low signal on T1WI, a high signal on T2WI, and no enhancement on contrast-enhanced T1WI. However, $T2^*$-GRE and SWI showed extensive cortical microbleeds, which were confirmed by biopsy [16]. Some scholars examined 9 patients with CAA; GRE detected 1146 CMBs, SWI detected 1432 CMBs. CMB scorers have better reliability with SWI (intraclass correlation coefficient, 0.87), but only moderate reliability with GRE (inter-class correlation coefficient, 0.52) [17]. SWI can not only detect CMBs, quantitatively detect iron changes, but also distinguish it from calcification [18]. In elderly patients with lacunar infarction, the SWI showed a higher positive rate for CMBs, followed by GRE-$T2^*$WI and other conventional sequences like T1WI, T2WI and T2FLAIR. To evaluate the effect of the modified GRE, Nandigam studied the relationship between the CMB detection rate and different sequences, section thickness and magnetic field strength in patients with CAA. With the other parameters unchanged, the positive rate of CMB is moderately increased if using SWI, having thinner sections and higher field strength. SWI is more likely to find CMBs with smaller diameters. In a regular thick slice, GRE only recognizes 33% of CMBs seen in thin slices by SWI [19, 20].

In SWI, artificial recognition of CMBs takes a long time, with limited reliability and reproducibility, which is prone to misdiagnosis. In order to solve that problem, researchers modified the software to improve the efficiency of diagnosis. Fazlollahi et al. proposed a computer-aided CMB detection technology based on machine learning with a new multi-scale Laplacian of Gaussian filtering approach. In 66 CMB patients, the CMBs were manually divided into two levels, "likely" or "confirmed", to verify the effectiveness of the method. Among the total population, the technology achieved 87% sensitivity and an average false detection rate of 27.1%. The sensitivity of the "confirmed" group was 93% and the false detection rate was 10% [21]. This is similar to another technique of automatic CMB detection based on independent subspace analysis and clustering [22]. SWI's automatic CMB detection technology improves reliability, reduces internal score variation and evaluation time, which is superior to existing technology and expected to improve expert screening efficiency.

In conclusion, for patients with CAA-related microbleeds, high-resolution SWI can achieve better diagnostic results, showing clear lesions and higher detection sensitivity.

Disclosure of conflict of interest

None.

Address correspondence to: Jiangwei Xie, Department of Radiology, Linyi Central Hospital, No.17 Jiankang Road, Yishui County, Linyi 276400, Shandong Province, China. Tel: +86-0539-2263342; E-mail: xiejiangwei09@126.com

References

[1] Skalski KA, Kessler AT and Bhatt AA. Hemorrhagic and non-hemorrhagic causes of signal loss on susceptibility-weighted imaging. Emergency Radiology 2018; 25: 691-701.

[2] Sharma R, Dearaugo S, Infeld B, O'Sullivan R and Gerraty RP. Cerebral amyloid angiopathy: Review of clinico-radiological features and mimics. J Med Imaging Radiat Oncol 2018; [Epub ahead of print].

[3] Kim SJ, Seo Y, Kim HJ, Na DL, Seo SW and Kim Y. Pathologically confirmed cerebral amyloid angiopathy with no radiological sign in a patient with early onset Alzheimer's disease. Yonsei Med J 2018; 59: 801-805.

[4] Zeng J, Zhao H, Liu Z, Zhang W and Huang Y. Lipopolysaccharide induces subacute cerebral microhemorrhages with involvement of nitric oxide synthase in rats. J Stroke Cerebrovasc Dis 2018; 27: 1905-1913.

[5] Caetano A, Ladeira F, Barbosa R, Calado S and Viana-Baptista M. Cerebral amyloid angiopathy - the modified boston criteria in clinical practice. J Neurol Sci 2018; 384: 55-57.

[6] De Reuck J, Maurage CA, Deramecourt V, Pasquier F, Cordonnier C, Leys D and Bordet R.

Aging and cerebrovascular lesions in pure and in mixed neurodegenerative and vascular dementia brains: a neuropathological study. Folia Neuropathol 2018; 56: 81-87.

[7] Jia C, Wei C, Hu M, Xu J, Niu K, Zhang C, Lv P, Li L and Dong Y. Correlation between antiplatelet therapy in secondary prevention of acute cerebral infarction and cerebral microbleeds: a susceptibility-weighted imaging (SWI) study. J Xray Sci Technol 2018; 26: 623-633.

[8] Noorbakhsh-Sabet N, Pulakanti VC and Z and R. Uncommon causes of cerebral microbleeds. J Stroke Cerebrovasc Dis 2017; 26: 2043-2049.

[9] Bulk M, Moursel LG, van der Graaf LM, van Veluw SJ, Greenberg SM, van Duinen SG, van Buchem MA, van Rooden S and van der Weerd L. Cerebral amyloid angiopathy with vascular iron accumulation and calcification. Stroke 2018; 49: 2081-2087.

[10] Sparacia G, Cannella R, Lo Re V, Gambino A, Mamone G and Miraglia R. Assessment of cerebral microbleeds by susceptibility-weighted imaging at 3T in patients with end-stage organ failure. Radiol Med 2018; 123: 441-448.

[11] Malhotra A, Schindler J, Mac Grory B, Chu SY, Youn TS, Matouk C, Greer DM and Schrag M. Cerebral microhemorrhages and meningeal siderosis in infective endocarditis. Cerebrovasc Dis 2017; 43: 59-67.

[12] Sparacia G, Agnello F, La Tona G, Iaia A, Midiri F and Sparacia B. Assessment of cerebral microbleeds by susceptibility-weighted imaging in Alzheimer's disease patients: a neuroimaging biomarker of the disease. Neuroradiol J 2017; 30: 330-335.

[13] Haacke EM, DelProposto ZS, Chaturvedi S, Sehgal V, Tenzer M, Neelavalli J and Kido D. Imaging cerebral amyloid angiopathy with susceptibility-weighted imaging. AJNR Am J Neuroradiol 2007; 28: 316-317.

[14] Yamada M. Cerebral amyloid angiopathy: emerging concepts. J Stroke 2015; 17: 17-30.

[15] Kusakabe K, Inoue A, Matsumoto S, Kurata M, Kitazawa R, Watanabe H and Kunieda T. Cerebral amyloid angiopathy-related inflammation with epilepsy mimicking a presentation of brain tumor: a case report and review of the literature. Int J Surg Case Rep 2018; 48: 95-100.

[16] Cheng AL, Batool S, McCreary CR, Lauzon ML, Frayne R, Goyal M and Smith EE. Susceptibility-weighted imaging is more reliable than T2*-weighted gradient-recalled echo MRI for detecting microbleeds. Stroke 2013; 44: 2782-2786.

[17] Buch S, Cheng YN, Hu J, Liu S, Beaver J, Rajagovindan R and Haacke EM. Determination of detection sensitivity for cerebral microbleeds using susceptibility-weighted imaging. NMR Biomed 2017; 30.

[18] Shao L, Wang M, Ge XH, Huang HD, Gao L and Qin JC. The use of susceptibility-weighted imaging to detect cerebral microbleeds after lacunar infarction. Eur Rev Med Pharmacol Sci 2017; 21: 3105-3112.

[19] Nandigam RN, Viswanathan A, Delgado P, Skehan ME, Smith EE, Rosand J, Greenberg SM and Dickerson BC. MR imaging detection of cerebral microbleeds: effect of susceptibility-weighted imaging, section thickness, and field strength. AJNR Am J Neuroradiol 2009; 30: 338-343.

[20] Renard D. Cerebral microbleeds: a magnetic resonance imaging review of common and less common causes. Eur J Neurol 2018; 25: 441-450.

[21] Bian W, Hess CP, Chang SM, Nelson SJ and Lupo JM. Computer-aided detection of radiation-induced cerebral microbleeds on susceptibility-weighted MR images. Neuroimage Clin 2013; 2: 282-290.

[22] Qi D, Hao C, Lequan Y, Lin S, Defeng W, Mok VC and Pheng Ann H. Automatic cerebral microbleeds detection from MR images via independent subspace analysis based hierarchical features. Conf Proc IEEE Eng Med Biol Soc 2015; 2015: 7933-7936.